Abdominal Radiology (2021) 46:1263–1271
https://doi.org/10.1007/s00261-020-02753-7

INTERVENTIONAL RADIOLOGY

Feasibility and safety of ultrasound-guided minimally invasive autopsy in COVID-19 patients

Olga R. Brook[1] · Kimberly G. Piper[2] · Noe B. Mercado[3] · Makda S. Gebre[3] · Dan H. Barouch[3] · Kathleen Busman-Sahay[4] · Carly E. Starke[4] · Jacob D. Estes[4] · Amanda J. Martinot[3,5] · Linda Wrijil[5] · Sarah Ducat[5] · Jonathan L. Hecht[6]

Received: 24 July 2020 / Revised: 30 August 2020 / Accepted: 3 September 2020 / Published online: 17 September 2020

Abstract

Objectives To determine the feasibility and safety of ultrasound-guided minimally invasive autopsy in COVID-19 patients.
Methods 60 patients who expired between 04/22/2020–05/06/2020 due to COVID-19 were considered for inclusion in the study, based on availability of study staff. Minimally invasive ultrasound-guided autopsy was performed with 14G core biopsies through a 13G coaxial needle. The protocol required 20 cores of the liver, 30 of lung, 12 of spleen, 20 of heart, 20 of kidney, 4 of breast, 4 of testis, 2 of skeletal muscle, and 4 of fat with total of 112 cores per patient. Quality of the samples was evaluated by number, size, histology, immunohistochemistry, and in situ hybridization for COVID-19 and PCR-measured viral loads for SARS-CoV-2.
Results Five (5/60, 8%) patients were included. All approached families gave their consent for the minimally invasive autopsy. All organs for biopsy were successfully targeted with ultrasound guidance obtaining all required samples, apart from 2 patients where renal samples were not obtained due to atrophic kidneys. The number, size, and weight of the tissue cores met expectation of the research group and tissue histology quality was excellent. Pathology findings were concordant with previously reported autopsy findings for COVID-19. Highest SARS-CoV-2 viral load was detected in the lung, liver, and spleen that had small to moderate amount, and low viral load in was detected in the heart in 2/5 (40%). No virus was detected in the kidney (0/3, 0%).
Conclusions Ultrasound-guided percutaneous post-mortem core biopsies can safely provide adequate tissue. Highest SARS-CoV-2 viral load was seen in the lung, followed by liver and spleen with small amount in the myocardium.

Keywords Autopsy · Biopsy · COVID-19

Abbreviations

COVID-19	Coronavirus 19
PCR	Polymerase chain reaction
SARS-CoV-2	Severe acute respiratory syndrome coronavirus 2
IRB	Institutional Review Board
HIPAA	Health Insurance Portability and Accountability Act of 1996
IHC	Immunohistochemistry

Electronic supplementary material The online version of this article (https://doi.org/10.1007/s00261-020-02753-7) contains supplementary material, which is available to authorized users.

✉ Olga R. Brook
obrook@bidmc.harvard.edu

[1] Department of Radiology, Beth Israel Deaconess Medical Center, Harvard Medical School, 330 Brookline Ave, Boston, MA 02215, USA

[2] Department of Vascular Surgery, Beth Israel Deaconess Medical Center, Boston, USA

[3] Center for Virology and Vaccine Research, Beth Israel Deaconess Medical Center, Harvard Medical School, Boston, MA 02215, USA

[4] Vaccine & Gene Therapy Institute and Division of Pathobiology and Immunology, Oregon National Primate Research Center, Oregon Health & Sciences University, Beaverton, OR 97006, USA

[5] Departments of Infectious Diseases and Global Health and Biomedical Sciences, Tufts University Cummings School of Veterinary Medicine, North Grafton, MA 01536, USA

[6] Department of Pathology, Beth Israel Deaconess Medical Center, Harvard Medical School, Boston, MA, USA

ISH	RNAscope in situ hybridization
ARDS	Acute respiratory distress syndrome
ESRD	End stage renal disease
SARS-N	SARS nucleocapsid protein

Introduction

In the setting of emerging infections, standard autopsy poses a risk to hospital staff and typically requires additional precautions [1]. Therefore, efforts to collect tissue for much needed research of COVID-19 have been significantly hampered [2]. Ultrasound-guided percutaneous core biopsies can provide tissue for research study in settings where biohazard precautions are difficult to implement [3–5]. Minimally invasive autopsy also limits body disfigurement so that patients' families may be more willing to consent to the procedure [6].

Here we report our experience with large tissue volume ultrasound-guided minimally invasive autopsy for research purposes in patients who died with SARS-CoV-2 coronavirus infection. Samples were assessed for quality and quantity of tissue obtained by ultrasound-guided percutaneous core biopsies using tissue weight, number of cores, preservation of tissue morphology by histology, and viral load as the metrics of performance. The histologic findings are compared to previously reported full autopsy findings in patients with COVID-19 [7–10].

Materials and methods

Ethics approval

Patients' families were consented for limited autopsies by a pathologist during a witnessed phone call immediately after the death after referral from the intensive care unit (ICU) team. Research using autopsy tissue for this project was approved by institutional IRB. A HIPAA waiver was granted by the institutional review board for access to the patients' charts for each project using the tissue. Tissue was provided to research teams per previously IRB-approved research protocols.

Patient population

Patients who expired in the intensive care units in our institution with SARS-CoV-2 infection between April 22 and May 6, 2020 were eligible to be included in the study. Autopsies were only performed during daytime weekday hours to accommodate staffing and contact with the family for consent. Five consecutive patients that expired in our institution's intensive care unit from COVID-19-related disease, during designated hours were included in this study. Minimally invasive ultrasound-guided autopsy was performed within 3 h of death to maintain tissue viability.

Ultrasound-guided minimally invasive autopsy procedure

Ultrasound-guided biopsies were performed by a board-certified diagnostic and interventional radiologist with 7 years of post-fellowship experience (ORB), who reviewed available pre-mortem diagnostic imaging studies prior to the autopsy for alteration to general anatomy that would preclude percutaneous biopsy access, such as depth of the organ from the skin surface, lack of the organ, replacement of normal tissue etc. The procedure was performed in the morgue on the standard morgue table in the supine position. The morgue is negative pressure room, vented outside to the building roof. Transfer of the body was performed while in the body bag and made easier in some patients when the body had been brought to the morgue on a metal tray rather than a hospital bed. The body bag was not opened until all personnel were wearing their protective gear. The body was not removed from the bag, and towels/drapes were tucked under either side of the body to protect the inner side of the bag. Radiologist, pathologist, and research assistant participating in the autopsy wore standard protective equipment used at autopsy that included yellow gown, eye shield, gloves, and shoe covers with the addition of an N95 mask. All protective equipment was donned prior to opening of the body bag. After autopsy, the body was wiped of water-soluble ultrasound gel, the towels/drapes were removed, and the bag was zipped and wiped with disinfectant before being placed back into the morgue cold room. Protective equipment was then doffed.

Standard donning and doffing of the protective equipment was performed, followed by washing hands with regular soap.

During the procedure, entry to the autopsy room was restricted to the radiologist, pathologist, and technician processing the samples.

Biopsies were obtained with direct ultrasound guidance with iU22 system (Philips Medical, Shelton, CT) with convex 5–1 MHz transducer for liver, spleen, kidney, and heart and linear 12–5 MHz transducer for lung, breast, and testicle specimens (Fig. 1). Fifteen preapproved research protocols requested a number of fresh frozen and formalin-fixed samples with total of 30 samples from the lung (10 fresh frozen and 20 in formalin), 20 samples from the liver (10 fresh frozen and 10 in formalin), 20 from the kidney (10 fresh frozen and 10 in formalin), 20 from the heart (10 fresh frozen and 10 in formalin), 12 from the spleen (5 fresh frozen and 7 in formalin), 4 from the subcutaneous fat (2 fresh frozen and 2 in formalin), 2 from the skeletal muscle (2 fresh frozen), 4 from the testis in males (2 fresh frozen and 2 in

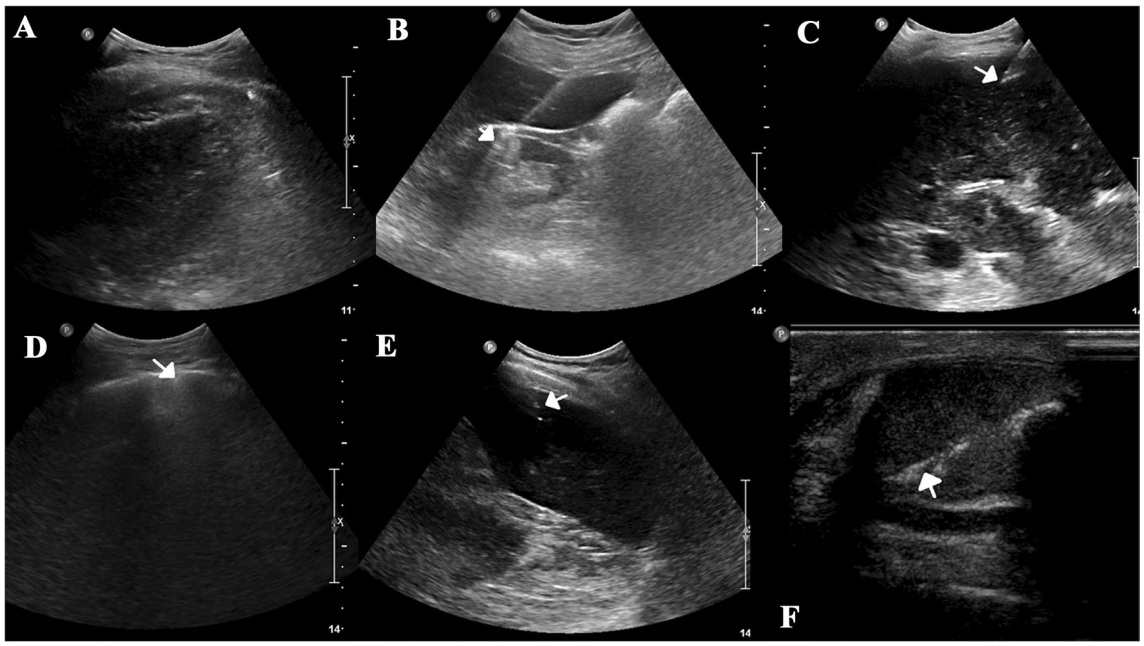

Fig. 1 Post-mortem ultrasound used for biopsy guidance. **a** Longitudinal image of the left ventricle in patient 1. **b** Transhepatic approach to the right kidney in patient 2. Tip of the needle is shown with white arrow. **c** Needle tip (arrow) in the right lobe of the liver, with the trajectory avoiding major vessels and large bile ducts. **d** Biopsy of the right lung parenchyma with the needle tip just beyond the pleura (arrow) in patient 1. **e** Biopsy of the spleen in patient 5 with arrow pointing to the tip of the needle. The trajectory of the biopsy is chosen to avoid hilar vessels. **f** Linear transducer was used to obtain the biopsy of the testes. Arrow pointing to the course of post-biopsy track in the testicular parenchyma

formalin), and 4 from breast tissue in females (2 fresh frozen and 2 in formalin) with total of 112 cores from each patient. Biopsies were obtained through 13G coaxial guide with 14 core biopsy Achieve system (Merit Medical, South Jordan, UT) with 20 mm sample length. Multiple core biopsies were acquired from each organ by tilting the coaxial needle a few degrees in different directions to avoid following the same path for all biopsies. The biopsies were not directed to target specific pathology.

In the *lung*, under direct ultrasound guidance and linear transducer, the needle tip of the coaxial needle was followed to the pleural surface in the right mid lung field from anterior mid-clavicular approach and then advanced additional 2 cm deep into the lung parenchyma. The needle could not be identified with ultrasound beyond the pleura (as expected due to comet tail/reverberation artifact caused by gas in the lung). In the *liver*, the coaxial needle was placed in the right lobe of the liver with trajectory avoiding large vessels and dilated biliary ducts, if present. In the *spleen*, the coaxial needle was directed away from the hilum with trajectory avoiding large vessels. In the *heart*, the coaxial needle was placed in the anterior left ventricle through the left anterior mid-clavicular or left parasternal chest wall. *Renal* cortex was targeted with patient in the supine position and coaxial needle coursing through the liver or intra-abdominal fat. In one patient, an obese patient was supported in a partial decubitus position to facilitate lateral access to the kidney. *Skeletal muscle* was obtained from the medial mid-thigh targeting quadriceps muscle. Subcutaneous abdominal *fat* was obtained in a superficial trajectory to avoid entering the muscles of the abdominal wall and peritoneum. The *testis* was targeted through the tunica into the testicular parenchyma in the longitudinal direction of the testes. *Breast* tissue was obtained adjacent to the nipple.

Tissue processing

During the course of the procedure, tissue was processed by a senior board-certified pathologist (JLH; 20 years of post-fellowship experience) using pre-labeled polypropylene cryovials (one core per vial) and containers of 10% buffered formalin (formalin-fixed cores were grouped in one container for each organ). Cryovials were immediately immersed in liquid nitrogen and then stored on dry ice until transfer to a – 80 °C freezer for distribution to research groups. Formalin-fixed tissue was considered to be non-infectious after 24 h and was processed in the clinical lab under the autopsy accession number created for each case. Frozen tissue was considered infectious and only distributed at the direction of the hospital biosafety officer.

Immunohistochemistry, RNAscope in situ hybridization, Quantitative RT-PCR, and subgenomic mRNA assay were

performed to assess preservation of viral RNA and determine tissue viral burden (Online Appendix 1) accordingly to previously described methods [11–13].

Results

None of three participants in the autopsy has shown any sign of illness nor met institutional criteria required for COVID testing during the study period and 6 weeks after cessation of the study.

Five patients were included in the study, 2 males and 3 females, with age range from 58 to 91 years with variety of comorbidities (Table 1). All patients underwent minimally invasive autopsy within 3 h of death with time between death and initiation of tissue collection at 120 min, 165 min, 150 min, 90 min, and 85 min. Limited hours of operation of this study resulted in approaching for consent 8% (5/60) of all patients that expired with COVID-19 in our institution in the study period. All families that were offered minimally invasive autopsy for their family member consented to and proceeded with the procedure.

Protocol-specified samples were obtained in almost all patients: lung (5/5, 100%), liver (5/5, 100%), spleen (5/5, 100%), kidney (3/5, 60%), heart (5/5, 100%), testes (2/2, 100%), breast (3/3, 100%), skeletal muscle (5/5, 100%), and fat (5/5, 100%), (Table 2). In total, in 3 patients in which all organs were successfully sampled 112 cores in each patient were obtained and in 2 patients in which kidney samples were not obtained 92 cores in each patient were obtained.

Weight of the samples for patient 3 was 15 mg for lung, 12 mg for liver, 20 mg for kidney, 13 mg for myocardium, and 18 mg for spleen. The specific tissue sampling was verified by gross examination of the cores for color and texture (Fig. 2) with spleen having a dark red color, heart, liver, and kidney having a tan color, and lung being heterogeneous white and red/hemorrhagic and spongy when added to liquid. Tissues were further verified the next day by histology. Samples of non-targeted fat tissue obtained inadvertently during the intervention were excluded based on the following criteria: fat was yellow, did not hold a cylindrical shape, and was easily smeared on a paper towel. Accidental sampling of the fat would indicate unintentional needle displacement and require ultrasound-guided repositioning of the coaxial needle prior to acquisition of additional samples.

In two patients with chronic end stage renal disease (patients 1 and 4), the kidneys were not targeted due to severe atrophy or extensive cystic changes in the kidneys and the high likelihood of non-diagnostic yield. In one patient, sampling of the heart was limited, although representative, because of altered anatomy with tissue cores including portions of stomach and lung, likely due to anterior pleural adhesions and hiatal hernia.

Table 1 Clinical characteristics and laboratory values for patients included in the cohort

	Age/gender	Hospital admission length (days)	Intubated	Comorbidities	Max temp (F)	LDH	D-Dimer	Total bili	ALT	AST	ALP	proBNP	cTropnT	CK-MB
1	91/M	10	No	ESRD on dialysis, h/o prostate ca, h/o PE, HTN	100	376	1174	0.4	11	35	66	8817	0.17	1
2	82/F	16	No	HTN, DM2, TIA, dementia	104.5	776	> 21,600	0.7	63	92	69	1686	0.08	1
3	58/F	40	Yes	HTN, DM2, obesity, mild CKD	101.3	542	> 21,600	0.4	70	378	156	1265	0.25	1
4	79/F	15	No	ESRD on dialysis, HTN	99.9	830	> 21,600	0.5	59	183	172	> 7000	0.23	4
5	75/M	31	Yes	Myasthenia gravis, HTN, AFib	102.8	880	20,937	3.5	173	105	185	Not obtained	1.35	25

Highest value during hospitalization is listed

HTN hypertension, *ESRD* end stage renal disease, *PE* pulmonary emboli, *DM2* diabetes mellitus type 2, *TIA* transient ischemic attack, *CKD* chronic kidney disease, *AFib* atrial fibrillation

Table 2 Summary of pathology, viral loads, immunohistochemistry (IHC), and RNAscope in situ hybridization (ISH) in five patients who expired due to COVID-19 (LOQ = Limit of quantification)

Pt	Specimen	Pathology	Viral loads in CoV N RNA copies/μg total RNA	Log10 viral loads genomic	Log10 viral load sub-genomic
1	Heart	Patchy replacement fibrosis, but no acute changes or inflammation	0	< LOQ	< LOQ
	Liver	Normal	7783	3.89	3.16
	Spleen	White pulp depletion and red pulp expansion	11	1.04	< LOQ
	Lung	Patchy pulmonary edema and acute alveolar hemorrhage; virus positive by IHC and ISH	60,311,200	7.78	< LOQ
2	Heart	Mild lymphocytic infiltrate between myocytes and around small vessels and rare microthrombus	10	1.00	3.52
	Liver	Central necrosis; virus positive by IHC	2	0.30	< LOQ
	Spleen	White pulp depletion and red pulp expansion and focal infarction	7	0.85	< LOQ
	Lung	Diffuse alveolar damage with septal lymphocytic infiltrate and type-II pneumocyte hyperplasia; virus positive by IHC and ISH	21,407	4.33	< LOQ
	Kidney	Acute tubular injury	0	< LOQ	< LOQ
3	Heart	Mild lymphocytic infiltrate between myocytes and around small vessels	0	< LOQ	< LOQ
	Liver	Periportal lymphocytic infiltrates	0	< LOQ	< LOQ
	Spleen	White pulp depletion and red pulp expansion	1	< LOQ	< LOQ
	Lung	Interstitial lymphocytic infiltrate and abundant alveolar macrophages	10	1.00	< LOQ
	Kidney	Acute tubular injury	0	< LOQ	< LOQ
4	Heart	Mild lymphocytic infiltrate between myocytes and around small vessels	120	2.08	3.25
	Liver	Unremarkable	2	0.30	< LOQ
	Spleen	White pulp depletion and red pulp expansion	32	1.51	< LOQ
	Lung	Patchy pulmonary edema and acute alveolar hemorrhage with prominent interstitial lymphocytic pneumonia with type-II pneumocyte hyperplasia and abundant alveolar macrophages; virus positive by IHC, ISH	17,413	4.24	< LOQ
5	Heart	Mild lymphocytic infiltrate between myocytes and around small vessels	0	0.00	2.95
	Liver	unremarkable	1	< LOQ	< LOQ
	Spleen	Necrotic due to infarction	0	< LOQ	< LOQ
	Lung	Diffuse alveolar damage and organizing alveolar hemorrhage; virus positive by IHC, ISH	8435	3.93	< LOQ
	Kidney	Tubular injury and acute inflammation and micro abscesses	0	< LOQ	< LOQ

Fig. 2 Gross appearance of samples of liver, lung, heart, spleen, and kidney

Due to large number of samples that needed to be obtained from each organ, the coaxial needle was slightly repositioned every few samples to prevent needle coursing through the same track and thereby maximize the yield of each core biopsy. Coaxial needle was utilized to prevent the need for repeated percutaneous access and targeting for each sample. Supine position of the patient made access to the kidney somewhat challenging due to its retroperitoneal location, especially in larger patients. In one patient, partial decubitus position improved ability to obtain renal samples.

Histopathological evaluation of the samples showed pathologies similar to those described in the published autopsy studies [7–10, 14], indicating that the random sampling was representative of COVID-19-related injury. Detailed description of patients' course and pathological findings are shown in Table 2 and Fig. 3. Characteristic findings in the lung included three patterns of injury, which were present heterogeneously throughout each core and among different cores. The dominant pattern in the lungs was pulmonary edema and fresh hemorrhage within alveolar spaces and minimal interstitial inflammation or edema. The second pattern was prominent interstitial chronic inflammation and edema, alveoli with type-II pneumocyte hyperplasia and multinucleation, and the third pattern was diffuse alveolar damage with organizing fibrin in alveolar spaces, and extending from alveolar septa, representing hyaline membranes. No intravascular microthrombi were identified distinct from the alveolar fibrin (Fig. 3). In several patients, the heart showed a pattern of viable myocardium with mild edema and a sparse lymphocytic infiltrate, predominantly around small vessels (Fig. 3). The spleen consistently showed increased red pulp with patchy necrosis or larger infarction, possibly related to shock. White pulp was diminished and sinusoids were filled with large activated lymphocytes (Fig. 2). The liver showed centrilobular necrosis (Fig. 3), and the kidney showed non-specific changes of acute tubular injury consistent with shock (Fig. 3). The histology of each patient was consistent with the clinical data (Online Appendix 2).

The *viral load* varied by organ (Table 2). All 5 patients (100%) had high levels of virus in their lung samples. Lower levels of virus were present in liver 4/5 (80%), spleen 4/5 (80%), and heart 2/5 (40%). There was no virus detected in the kidney samples (0/3, 0%).

Immunohistochemistry and RNAscope in situ *hybridization* for viral nucleocapsid protein showed staining in 4 of 5 cases (case 3 was negative). Likely explanation for lack of nucleocapsid staining while having a viral load detected is due to long course of disease in this patient. This patient likely succumbed to complications of the COVID and not during initial infection. Staining was predominantly in the lung (Fig. 4), where viral loads were also very high

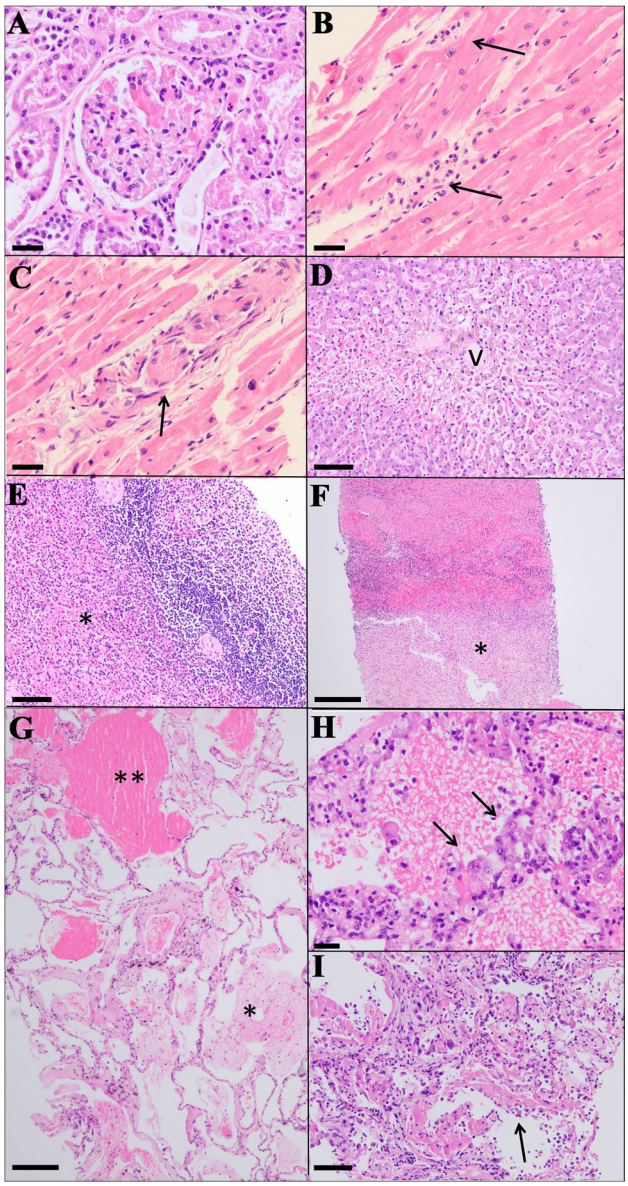

Fig. 3 Histology. Kidney (**a**, patient 2) showing well-preserved glomeruli and tubular epithelium with acute injury. Heart showing viable myocardium with mild edema and lymphocytic infiltrate (arrow) around small vessels (**b**, patient 3) and a small thrombosed myocardial vessel (**c**, patient 2, arrow). Liver section showed normal portal tracts, but necrosis around the central vein (v), consistent with septic shock (**d**, patient 2). Spleen (patient 2) showing increased red pulp (**e**,*), lymphocyte depletion, and areas of infarction (**f**,*). Lungs showed pulmonary edema (**g**,*, patient 1) and patchy alveolar hemorrhage (**g**,**), type-II pneumocyte hyperplasia (**h**, arrow,), and hyaline membranes of ARDS (**i**, arrow, patient 2). (Hematoxylin- and eosin-stained sections. Scale bars indicate: Panel **a**–**c** and **e** = 100 microns, **d**, **e** and **i** = 200 microns, **f**, **g** = 500 microns)

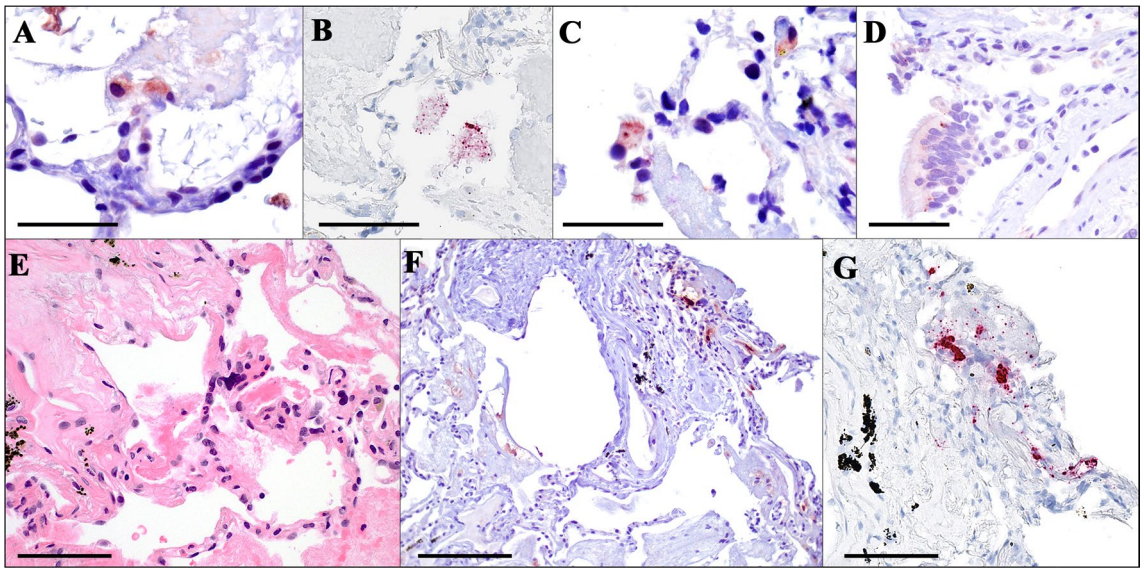

Fig. 4 Detection of SARS-N nucleocapsid by Immunohistochemistry (IHC) and RNAscope in situ hybridization (ISH) in the lung. IHC (**a**) and ISH (**b**) highlight desquamated alveolar pneumocytes. Bronchial epithleial cells were variably positive by IHC (**c**, **d**). The same pattern was seen on ISH (not shown). An area of ARDS (**e**, H&E stain) with IHC (**f**) and ISH (**g**) highlighting alveolar lining cells and macrophages trapped in fibrin. (Case 1, original magnification, ×400, Scale bar = 100 um)

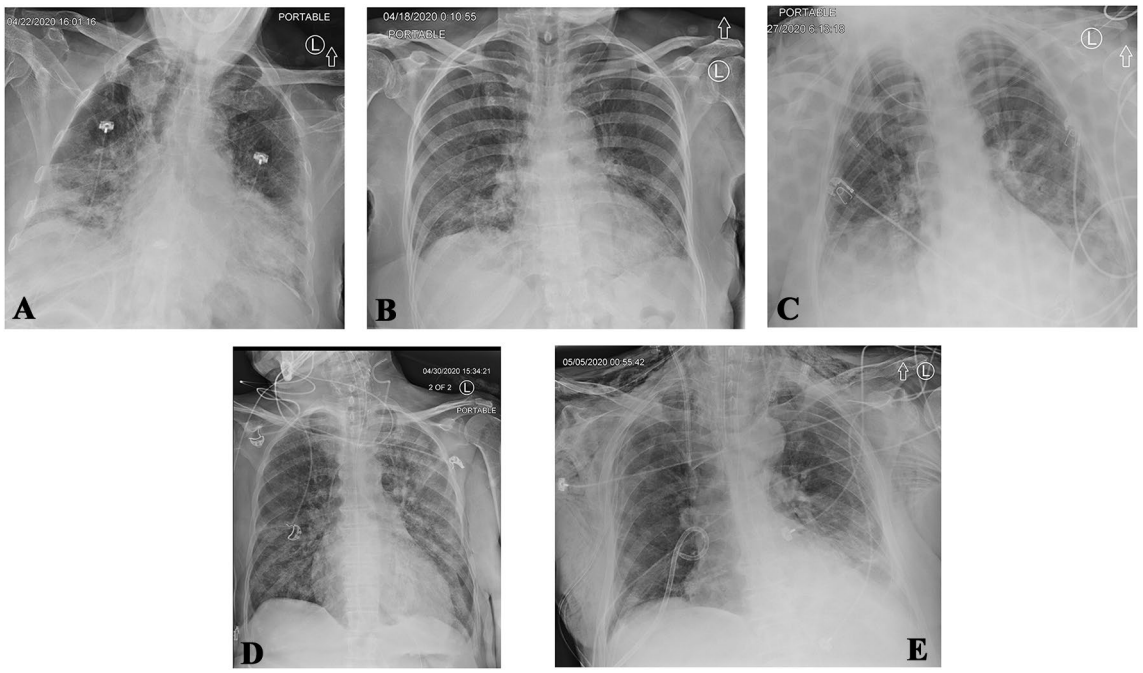

Fig. 5 Chest X-ray in patient 1 obtained a day prior to death showed diffused patchy bilateral opacities and cardiac enlargement, which were new compared to X-ray a week prior (**a**). Chest X-ray performed 6 days prior to death showed persistent bibasilar airspace opacities (**b**). Similarly, chest X-ray obtained a day prior to death in patient 3 showed bilateral airspace opacities (**c**). Chest X-ray obtained a day prior to death in patient 4 showed extensive perihilar and lower lobe bilateral consolidations, progressed from prior (**d**). Chest X-ray obtained a day prior to death in patient 5 showed left lower lung consolidation and subcutaneous emphysema, s/p chest tube for right pneumothorax (**e**)

(Table 2). One case showed focal staining in the sinusoids of the liver.

Immediate pre-mortem imaging was sparse, and included chest X-rays (Fig. 5) that showed bilateral predominantly basilar airspace opacities.

Discussion

We have shown the safety and good diagnostic quality of core tissue sampling for research purposes in COVID-positive patients using a minimally invasive ultrasound-guided approach. We were able to obtain all required samples from the variety of organs within 3 h of death, with preservation of tissue quality for histology and ancillary research studies.

Our results regarding tissue quality are comparable to prior reports of minimally invasive autopsy of tumor tissues obtained under computerized tomography guidance by Van Der Linden et al. [15]. In that study, they found that tissue quality for RNA analysis of flash frozen core samples was comparable to open autopsy, and declined with post-mortem interval. Their best results were from tissue taken within 3 h of death. In our study, the time of acquisition ranged from 85 to 165 min but shortened with each consecutive patient as more experience was gained. Time to snap freezing and formalin fixation was shorter since tissue was processed during the case.

Despite limited and non-lesion-directed sampling, the histology was consistent with those described in COVID-19 patients [7–10, 14], including pulmonary edema and hemorrhage with diffuse alveolar damage, sparse lymphocytic infiltrate around small vessels in the myocardium, increased splenic red pulp with patchy necrosis, and centrilobular necrosis in the liver. The small number of patients, lack of comparison group, and presence of comorbidities makes it impossible to directly relate the findings to solely COVID-19 infection based on this small study.

Although not commonly used, minimally invasive autopsy has previously been shown to provide similar diagnostic results and tissue for ancillary testing to the traditional autopsy [4, 5, 16]. As shown in our study, minimally invasive approach appears to be a viable alternative in high-risk settings for patients with infectious diseases in absence of adequate protection to the morgue staff [1]. This approach has been used previously in a recent outbreak of Yellow Fever in Brazil [3], as well as in prior studies from Mozambique with variety of infectious etiologies [16, 17]. One previous COVID-19-related autopsy study using ultrasound-guided core biopsies has been reported, but was limited to lungs, liver, and heart, and did not include details about the imaging or tissue volume obtained [9].

SARS-CoV-2 viral loads of the freshly frozen tissue samples provided additional insight into the spread of the virus in the body. Highest concentrations of the virus were seen in the lungs, with small to moderate amount of virus in the liver, spleen, and heart. No virus was detected in the kidneys. This is surprising given the degree of renal failure in these patients. Viral infection of proximal tubules has been described [18]. It appears that obtaining viral loads is safe and feasible with minimally invasive biopsy from variety of organs.

Our study has a number of limitations. The number of patients included was small due to recruitment being constrained by staffing availability during a time when hospitals were at high census due to the pandemic. The urgency of providing research scientists with sufficient tissue for investigation in a safe manner during an ongoing pandemic was the main priority of this study. Interestingly, not a single patients' family declined the minimally invasive autopsy approach, potentially indicating a high level of acceptance as the procedure does not cause body disfigurement [6]. It is reassuring that the protocol in this study was found to be safe for personnel but this would need to be confirmed by larger studies. Other limitations include lack of assessment of the level of experience required to obtained sufficient quality tissue. Only a single experienced radiologist and pathologist participated in this study. It is possible that without this expertise the results would be less successful and additional training would be required.

Post-mortem ultrasound guidance has inherent limitations. First, residual air in the aerated lung does not allow tracking the needle beyond the pleura. Therefore, the needle was tracked to the pleura and then the trajectory was extrapolated for additional 2 cm into lung parenchyma. Kidney can be difficult to target from the anterior approach in the supine position due to its retroperitoneal location. Partial decubitus on the autopsy table facilitated access to the kidney. Large body habitus and pre-existing conditions (e.g., pneumothorax, small kidneys in ESRD) may complicate ultrasound guidance further, but this could be overcome with review of pre-mortem imaging, if it was obtained. Bowel and mesentery can be visualized by ultrasound, but these structures are thin and not amenable to a needle biopsy, and therefore, we have not attempted to sample these structures. Brain and blood vessels are not amenable for percutaneous ultrasound-guided biopsy, and thus, these structures needs to be evaluated by full traditional autopsy when it is required. Access to the heart was limited in one patient by overlying lung/pleural adhesions. Onsite visual evaluation of the gross core samples ensured that adequate tissue rather than fat was obtained. Lastly, major limitation of this study is small number of patients included. Future studies with larger number of patients and correlation with full traditional autopsy would be helpful to confirm whether minimally invasive autopsy provides a sufficiently representative sample.

In conclusion, we have shown that minimally invasive ultrasound-guided autopsy is feasible and safe to obtain large number of samples from multiple organs in COVID-19 patients for research purposes.

Acknowledgements We are grateful to Dr Deb Burstein for her comments in reviewing the manuscript.

Compliance with ethical standards

Conflict of interest All authors have no conflicts of interest to declare.

References

1. Hanley B, Lucas SB, Youd E, Swift B, Osborn M. Autopsy in suspected COVID-19 cases. J. Clin. Pathol. 2020;73. https://doi.org/10.1136/jclinpath-2020-206522.
2. Ledford H. Autopsy slowdown hinders quest to determine how coronavirus kills. Nature 2020. https://doi.org/10.1038/d41586-020-01355-z.
3. Duarte-Neto AN, Monteiro RA de A, Johnsson J, Cunha MDP, Pour SZ, Saraiva AC, et al. Ultrasound-guided minimally invasive autopsy as a tool for rapid post-mortem diagnosis in the 2018 Sao Paulo yellow fever epidemic: Correlation with conventional autopsy. PLoS Negl Trop Dis 2019;13. https://doi.org/10.1371/journal.pntd.0007625.
4. Fan JKM, Tong DKH, Poon JTC, Lo OS, Beh PS, Patil NG, et al. Multimodality minimally invasive autopsy-A feasible and accurate approach to post-mortem examination. Forensic Sci Int 2010;195:93–98.
5. Fariña J, Millana C, Fdez-Aceñero JM, Furio V, Aragonvillo P, Martin VG, et al. Ultrasonographic autopsy (echopsy): A new autopsy technique. Virchows Arch 2002;440:635–639.
6. Maixenchs M, Anselmo R, Zielinski-Gutiérrez E, Odhiambo FO, Akello C, Ondire M, et al. Willingness to Know the Cause of Death and Hypothetical Acceptability of the Minimally Invasive Autopsy in Six Diverse African and Asian Settings: A Mixed Methods Socio-Behavioural Study. PLoS Med 2016;13. https://doi.org/10.1371/journal.pmed.1002172.
7. Yao XH, Li TY, He ZC, Ping HW, Yu SC, Mou HM, et al. [A pathological report of three COVID-19 cases by minimally invasive autopsies]. Zhonghua bing li xue za zhi = Chinese J Pathol 2020;49:E009.
8. Bradley BT, Maioli H, Johnston R, Chaudhry I, Fink SL, Xu H, et al. Histopathology and Ultrastructural Findings of Fatal COVID-19 Infections. medRxiv 2020;:2020.04.17.20058545.
9. Tian S, Xiong Y, Liu H, Niu L, Guo J, Liao M, et al. Pathological study of the 2019 novel coronavirus disease (COVID-19) through postmortem core biopsies. Mod Pathol 2020. https://doi.org/10.1038/s41379-020-0536-x.
10. Fox SE, Akmatbekov A, Harbert JL, Li G, Brown JQ, Heide RSV, et al. Pulmonary and Cardiac Pathology in Covid-19: The First Autopsy Series from New Orleans. medRxiv 2020;:2020.04.06.20050575.
11. Chandrashekar A, Liu J, Martinot AJ, McMahan K, Mercado NB, Peter L, et al. SARS-CoV-2 infection protects against rechallenge in rhesus macaques. Science (80-) 2020;:eabc4776.
12. Deleage C, Wietgrefe SW, Del Prete G, Morcock DR, Hao XP, Piatak Jr M, et al. Defining HIV and SIV Reservoirs in Lymphoid Tissues. Pathog Immun 2016;1:68.
13. Wölfel R, Corman VM, Guggemos W, Seilmaier M, Zange S, Muller MA, et al. Virological assessment of hospitalized patients with COVID-2019. Nature 2020;581:465–469.
14. Ackermann M, Verleden SE, Kuehnel M, Haverich A, Welte T, laenger F, et al. Pulmonary Vascular Endothelialitis, Thrombosis, and Angiogenesis in Covid-19. N Engl J Med 2020;:NEJMoa2015432.
15. Van Der Linden A, Blokker BM, Kap M, Weustnik AC, Robertus JL, Riegman PH, et al. Post-mortem tissue biopsies obtained at minimally invasive autopsy: An RNA-quality analysis. PLoS One 2014;9. https://doi.org/10.1371/journal.pone.0115675.
16. Castillo P, Martínez MJ, Ussene E, Jordao D, Lovane L, Ismail MR, et al. Validity of a Minimally Invasive Autopsy for Cause of Death Determination in Adults in Mozambique: An Observational Study. PLoS Med 2016;13. https://doi.org/10.1371/journal.pmed.1002171.
17. Martínez MJ, Massora S, Mandomando I, Ussene E, Jordao D, Lovane L, et al. Infectious cause of death determination using minimally invasive autopsies in developing countries. Diagn Microbiol Infect Dis 2016;84:80–86.
18. Batlle D, Soler MJ, Sparks MA, Hiremath S, South AM, Welling PA, et al. Acute Kidney Injury in COVID-19: Emerging Evidence of a Distinct Pathophysiology. J Am Soc Nephrol 2020. https://doi.org/10.1681/asn.2020040419.